

# Direct electrochemistry and electroanalysis of hemoglobin adsorbed in self-assembled films of gold nanoshells

Yi Wang<sup>a,b</sup>, Weiping Qian<sup>a,\*</sup>, Yong Tan<sup>a</sup>, Shaohua Ding<sup>a</sup>, Haiqian Zhang<sup>c</sup>

<sup>a</sup> State Key Laboratory of Bioelectronics, Department of Biological Science and Medical Engineering, Southeast University, Nanjing 210096, PR China

<sup>b</sup> School of Chemistry and Chemical Engineering, Southeast University, Nanjing 210096, PR China

<sup>c</sup> College of Materials Science and Technology, Nanjing University of Aeronautics and Astronautics, Nanjing 210016, PR China

Received 18 December 2006; received in revised form 31 December 2006; accepted 6 January 2007

Available online 18 January 2007

## Abstract

Gold nanoshells (GNSs), consisting of a silica core and a thin gold shell, were self-assembled on the surface of 3-aminopropyltrimethoxysilane (APTES) modified indium tin oxide (ITO) electrode. The resulting novel GNSs-coated ITO (GNSs/APTES/ITO) electrode could provide a biocompatible surface for the adsorption of hemoglobin (Hb). The UV-visible (UV-vis) spectra indicated that Hb adsorbed on the GNSs interface retained the native structure. Electrochemical impedance spectra and cyclic voltammetric techniques were employed to evaluate the electrochemical behaviors of Hb, the results demonstrated that GNSs could act as electron tunnels to facilitate electron transfer between Hb and the electrode. Based on the activity of Hb adsorbed on the GNSs/APTES/ITO electrode toward the reduction of hydrogen peroxide, a mediator-free H<sub>2</sub>O<sub>2</sub> biosensor was constructed, which showed a broad linear range from 5 μM to 1 mM with a detection limit of 3.4 μM (S/N = 3). The apparent Michaelis–Menten constant was calculated to be 180 μM, suggesting a high affinity.

© 2007 Published by Elsevier B.V.

**Keywords:** Gold nanoshells; Metal nanoparticles; Hemoglobin; Direct electrochemistry; Electrocatalysis; Hydrogen peroxide

## 1. Introduction

Incorporation of metal nanoparticles (MNPs) into electrochemical applications has attracted extensive interest owing to their extraordinary catalytic properties and their interface-dominated properties over bulk-metal electrodes. These MNPs-modified electrodes have been focused on studying the direct electrochemistry of protein, especially heme protein (such as cytochrome *c* [1,2], hemoglobin (Hb) [3–5], myoglobin [6,7], horseradish peroxidase [8,9] and so on), and further applications in mediator-free biosensors and catalysis [10,11]. Many kinds of metal and their oxide nanoparticles, such as Au, Ag, Pt, TiO<sub>2</sub>, Fe<sub>3</sub>O<sub>4</sub>, ZrO<sub>2</sub> and MnO<sub>2</sub> nanoparticles, were imposed to catalyze electrochemical reaction and enhance the electron transfer between enzyme and electrodes. For example, Willner and co-workers [12] incorporated gold nanoparticles (GNPs) into apo-glucose oxidase and constructed the glucose biosen-

sor, which exhibited seven times faster of the electron transfer between the enzyme redox centre and the electrode than that between glucose oxidase and its natural substrate, oxygen. Caruso and co-workers [13] fabricated dense GNPs films by the hybrid of GNPs in polyelectrolyte multilayers, and revealed that GNPs could improve the electron-transfer characteristics of the films and they further utilized the films as high-sensitive electrochemical sensors for nitrous oxide. Recently, Hempelmann and co-workers [14] fabricated highly ordered macroporous gold films for increasing electroenzymatic oxidation of glucose with glucose dehydrogenase.

Many researches have been focused on the electrochemical applications of single-component nanoparticles including single-component MNPs or nonmetal nanoparticles such as SiO<sub>2</sub> nanoparticles [15]. However, the electrochemical properties of composite nanoparticles, which are not completely similar to single-component nanoparticles, have not been studied clearly. Recently, the composite nanoparticle of GNS, consisted of a silica core covered by a thin gold shell, was studied in many application fields, such as drug delivery [16], tissue repair [17], contrast agents for imaging [18], cancer

\* Corresponding author. Tel.: +86 25 83795719; fax: +86 25 83795719.

E-mail address: [wqian@seu.edu.cn](mailto:wqian@seu.edu.cn) (W. Qian).

therapy [19], surface enhanced Raman scattering (SERS) [20], immunoassay [21] and so on. These significant applications could not only ascribe to their unique chemical, physical properties and good biocompatibility, but also to their controllable resonance peak over a broad region ranging from the near-UV to the mid-infrared. However, there are no reports on the electrochemical properties of the GNSs-modified electrodes, and the electrochemical behaviors of redox protein adsorbed on the GNSs-modified electrodes are not yet understood in detail.

In this paper, GNSs were constructed on the surface of APTES-modified ITO (APTES/ITO) electrode by the self-assembly technique to form GNSs/APTES/ITO electrode. This self-assembled GNSs film could provide large surface area, superior conductivity and favorable microenvironment for retaining the biological activity of the adsorbed hemoglobin (Hb) and facilitate the direct electron transfer between the Hb and the ITO electrode, as confirmed by electrochemical and attenuated UV–vis spectroscopy. The electrochemical behavior of Hb was discussed in detail, and an effective  $\text{H}_2\text{O}_2$  biosensor was constructed.

## 2. Experimental

### 2.1. Reagents and materials

Bovine hemoglobin (Hb, MW 64,500) and 3-aminopropyltrimethoxysilane (APTES, 97%) were purchased from Sigma, and tetraethoxysilane (TEOS, 98%) was purchased from Alfa Aesar, hydrogen tetrachloroaurate(III) hydrate, hydrogen peroxide ( $\text{H}_2\text{O}_2$ , 30%), potassium carbonate ( $\text{K}_2\text{CO}_3$ , 99%), sodium borohydride ( $\text{NaBH}_4$ ), formaldehyde and ethanol (99%) were purchased from Nanjing Sunshine Biotechnology Ltd., China. All chemicals were used as received. Silica colloids ( $\sim 110$  nm in diameter) were obtained from Nissan of Japan. ITO glasses ( $< 200 \Omega/\text{cm}^2$ ) were purchased from Xiamen ITO Photoelectricity Industry Co., Ltd. of China. Triply distilled water was used in our experiments.

### 2.2. Preparation of GNSs

GNSs were prepared according to the method described by Halas and co-workers [22] with some modifications, as reported in our previous work [23,24]. Silica colloids were purified by centrifuging and redispersing for five times in ethanol. And then 0.275 mL of APTES was added to 35 mL of purified silica colloids (0.12 g/mL in ethanol) under vigorous magnetic stirring at  $45^\circ\text{C}$  for 3 h. APTES-functionalized silica colloids were purified by centrifuging and redispersing in ethanol. On the other hand, GNPs with an average diameter of 2–5 nm were prepared as reported in our previous work [25,26]. APTES-functionalized silica colloids ( $\sim 5.3 \times 10^{11}$  particles/mL in ethanol) were added dropwise to the 200 mL of gold sol under vigorous magnetic stirring (600 rpm) to form gold-attached silica colloids (Au/SiO<sub>2</sub> nanoparticles). After centrifugation and removing the supernatant for three times, 200 mL of Au/SiO<sub>2</sub> nanoparticles were redispersed in 45 mL of water.

Under continuous stirring, various amounts of gold-attached silica colloids were added to 60 mL of the aged  $\text{HAuCl}_4/\text{K}_2\text{CO}_3$  solution, followed by 0.15 mL of formaldehyde to form the GNSs [23]. The amount of the added gold-attached silica colloids was depended on the intended thickness of the gold shells. In this process, the color of the suspension changed from colorless over violet and blue to a strongly scattering brown solution. The suspensions were centrifuged to concentrate the GNSs for further use and to remove excess reagents.

### 2.3. Modification of ITO electrode

A sheet of ITO was sonicated in detergent solution, triply distilled water, acetone and ethanol for 15 min, respectively. After dried with a stream of high purity nitrogen, the substrate was immersed in an ethanol solution of 1% (v/v) APTES for 30 min at  $75^\circ\text{C}$ , rinsed five times in ethanol with sonication, and dried at  $120^\circ\text{C}$  for 3 h. The silanized ITO was subsequently immersed overnight in GNSs solution ( $\sim 1.24 \times 10^{11}$  particles/mL in water) to form the GNSs/APTES/ITO electrode. After that the modified ITO electrode was dried by nitrogen.

### 2.4. The adsorption of Hb to GNSs/APTES/ITO electrodes

GNSs/APTES/ITO electrodes were immersed in 0.1 M phosphate buffer solution (PBS, pH 7.0) containing 5 mg/mL Hb at  $4^\circ\text{C}$ . After incubated for 12 h, the modified electrodes were thoroughly rinsed with triply distilled water. They were stored in PBS solution at pH 7.0 and  $4^\circ\text{C}$  until use.

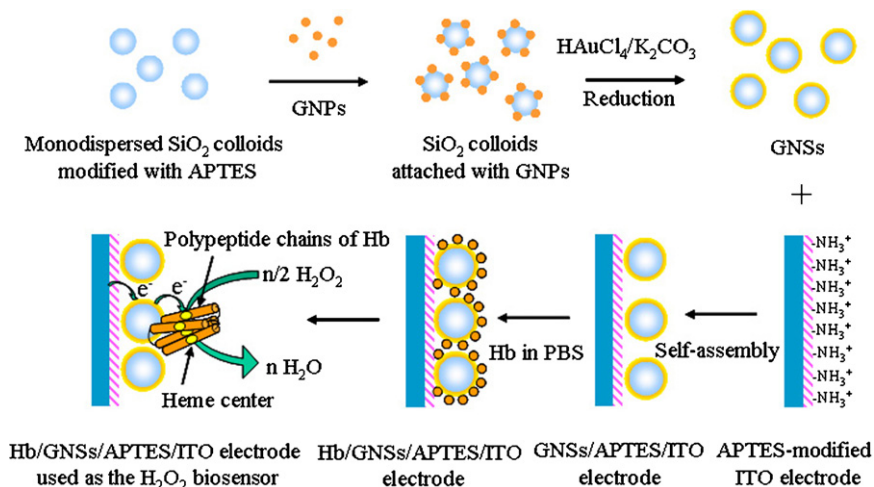
### 2.5. Characterization

All electrochemical experiments were carried out on a CHI650b electrochemical workstation (CH Instruments, USA) in a conventional one-compartment cell. The standard three-electrode system was used for measurements. A saturated calomel electrode was used as the reference electrode, a Pt wire was used as the counter electrode, and the bare ITO electrode or modified ITO electrode with an exposed geometric area of ca.  $0.12 \text{ cm}^2$  was employed as the working electrode. A JEM2000EX transmission electron microscopy (TEM) was used to collect the image of GNSs. SEM characterization was carried out on a LEO 1530 VP SEM to image the morphology of the GNSs/APTES/ITO electrode. UV–vis spectra were employed to investigate the plasmon resonance band of GNSs and the Soret band of Hb by using a Shimadzu UV3150 UV–vis spectrophotometer in a transmission mode. Modified ITO electrode was measured by mounting it (upright to the incidence of light) in the sample cell of the spectrophotometer with a bare ITO electrode in the reference cell.

## 3. Results and discussion

### 3.1. Preparation and characterization of the GNSs/APTES/ITO electrode

Scheme 1 represents the fabrication procedures for a GNSs/APTES/ITO electrode. As shown in the inset A of Fig. 1,



Scheme 1. Fabrication procedures for a GNSs/APTES/ITO electrode, the process of Hb adsorption on its surface, the electron transfer between the heme center of Hb and the ITO electrode via GNSs, and the H<sub>2</sub>O<sub>2</sub> biosensor.

GNSs were fabricated with shell thickness of  $\sim 25$  nm, which was estimated according to the known size ( $\sim 110$  nm in diameter) of silica core. GNSs can be assembled on the APTES/ITO electrode by complexation between GNSs and the amino groups [26], as shown in the inset B of Fig. 1. The plasmon resonance peak of GNSs dispersed in water was significantly at 725 nm. After assembled on ITO electrode, the resonance peak of GNSs was 660 nm in air, as shown in Fig. 1. The blue shift of resonance peak was mainly ascribed to the change of the environmental refractive index. These data indicate that the GNSs had been assembled successfully on the APTES-modified ITO electrode. The stability of the GNSs on ITO electrode was studied by inserting the GNSs/APTES/ITO electrode into the cuvettes filled with water, ethanol and benzene in turn prior to perform the spectral measurements. The analysis by the UV–vis spectra (data not shown) shows no discernible difference between pre- and post-immersing, suggesting that the solvents did not cause the GNSs to detach from the ITO glass substrate.

The GNSs/APTES/ITO electrodes were characterized electrochemically in 0.5 M H<sub>2</sub>SO<sub>4</sub> at a scan rate of 0.1 V/s. The cyclic voltammograms of GNSs/APTES/ITO electrode exhibits the characteristic peaks with an oxidation peak starting at 1.1 V in the positive scan and a reduction peak at 0.8 V in the reverse scan, whereas no Faradaic current responds on the bare ITO electrode, as shown in Fig. 2. The appearance of obvious redox peaks exhibited on the GNSs/APTES/ITO electrode was mainly ascribed to their great real surface area. And the reduction peak at 0.8 V can be attributed to the reduction of the gold oxide formed during the anodic cycle. The charge density associated with the reductive process is 0.707 mC/cm<sup>2</sup> for the GNSs/APTES/ITO electrode, as shown in Fig. 2b, with R.S.D. value of 3.69% for four independent electrodes. This result shows that the electrode area of the GNSs adsorbed on ITO electrode is 1.83 times higher than that of the planar Au electrode (assuming that the reduction of a monolayer of gold oxide requires 0.386 mC/cm<sup>2</sup>) [27]. Assuming that all of the GNSs surfaces are involved in the electrochemical reaction, the surface coverage of the GNSs

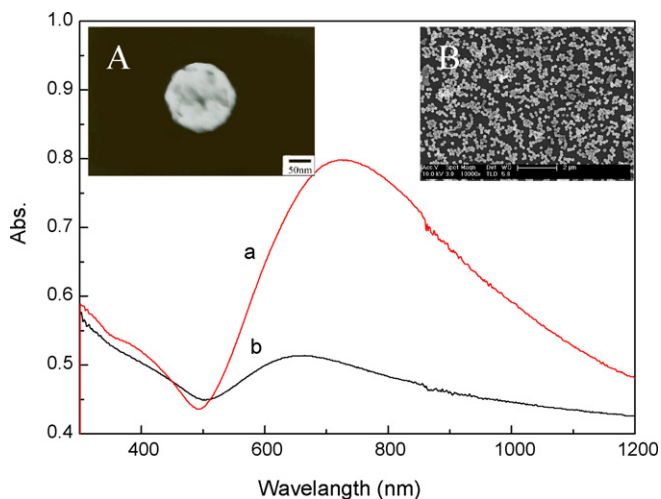


Fig. 1. UV–vis absorption spectra of GNSs (a) dispersed in water and (b) assembled on ITO electrode in air. Inset A: A TEM image of a GNS (the scale bar is 50 nm). Inset B: A SEM image of GNSs assembled on the surface of ITO (the scale bar is 2 μm).

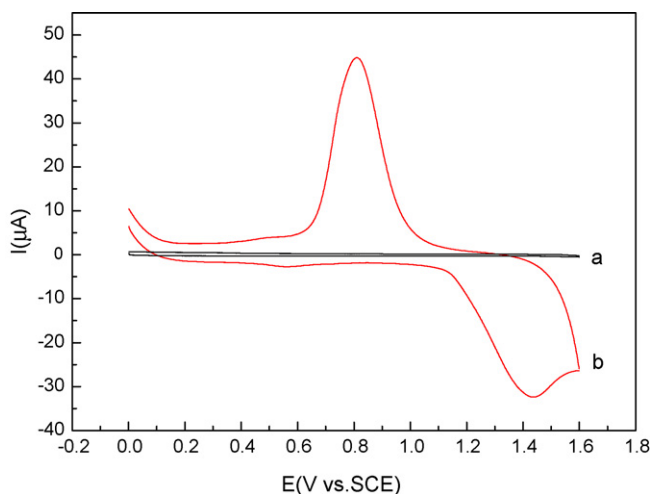


Fig. 2. Cyclic voltammograms of (a) bare ITO and (b) GNSs/APTES/ITO electrodes in 0.5 M H<sub>2</sub>SO<sub>4</sub> at 0.1 V/s.

is estimated to be ca.  $2.28 \times 10^9$  particles/cm<sup>2</sup>, which is little higher than the number estimated with the SEM image (the inset B of Fig. 1). This may be ascribed to the rough and unshaped surface of the gold shells.

### 3.2. Adsorption of Hb on GNSs/APTES/ITO electrodes

After immersion of the GNSs/APTES/ITO electrode in a solution containing Hb, this protein can be adsorbed on the GNSs surface by the interactions between the cysteine or NH<sub>4</sub><sup>+</sup>-lysine functional groups of the Hb and the GNSs. Fig. 3 shows the UV–vis absorption spectra of the GNSs/APTES/ITO electrode before and after incubation of Hb for 12 h in PBS (pH 7.0) solution, and the absorption peak at 407 nm (Fig. 3c) was attributed to the Soret band [28] of Hb adsorbed on the surface of GNSs. Previous studies have demonstrated that the absorption band would diminish upon the native protein denaturation [29], and UV–vis spectroscopy is an effective means to probe the characteristic structure of proteins [30–32]. Compared with the absorption peak of native Hb in PBS solution (Fig. 3a), the same absorption peak at 407 nm of Hb adsorbed on GNSs demonstrates that the adsorbed Hb molecules retain their native structure [33,34]. Furthermore, the data in Fig. 3 shows that the plasmon resonance peak of GNSs on ITO electrode shifts little after the adsorption of Hb, indicating that the adsorption of Hb did not influence the stability of GNSs.

Cyclic voltammetry of an electroactive species such as K<sub>3</sub>[Fe(CN)<sub>6</sub>] is a valuable convenient tool for testing the kinetic barrier of the interface because the electron transfer between solution species and the electrode must occur by tunneling either through the barrier or through the defects in the barrier. Therefore, it was chosen as a marker to investigate the changes of electrode behavior after each assembly step. Fig. 4 shows the cyclic voltammograms of differently modified electrodes in 0.1 M PBS (pH 7.0) containing 5 mM K<sub>3</sub>[Fe(CN)<sub>6</sub>]. As expected, ferricyanide exhibits quasi-reversible behavior on a bare ITO electrode (Fig. 4a) with a peak-to-peak separation ( $\Delta E_p$ ) of 0.28 V at a scan rate of 0.1 V/s. At the GNSs/APTES/ITO electrode, a little decrease in the redox peak and the  $\Delta E_p$  was widened to 0.35 V, which may be due to the electrostatic repulsion between Fe(CN)<sub>6</sub><sup>3-</sup> or Fe(CN)<sub>6</sub><sup>4-</sup> anion and the negatively charged surface of GNSs. This electrostatic repulsion would hinder the diffusion of ferricyanide toward the electrode interface and slacked the electron-transfer kinetics [35]. And the great widening of  $\Delta E_p$  at the Hb adsorbed GNSs/APTES/ITO electrode mainly ascribes to its large impedance.

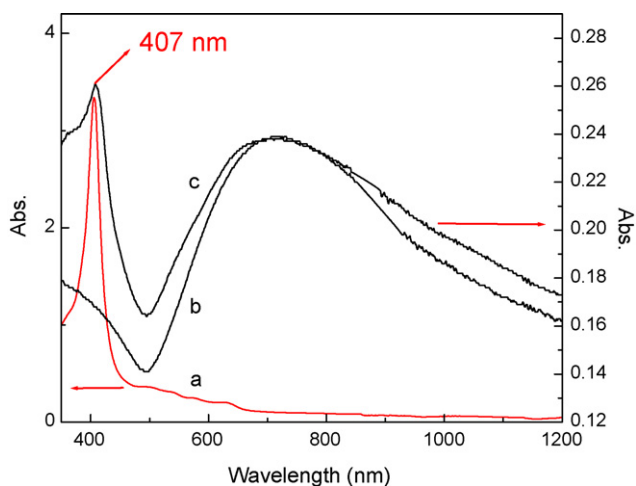


Fig. 3. UV–vis absorption spectra of (a) 0.5 mg/mL Hb in PBS (pH 7.0), (b) the GNSs/APTES/ITO electrode in PBS (pH 7.0) and (c) the GNSs/APTES/ITO electrode after incubating for 12 h in PBS (pH 7.0) containing Hb (5 mg/mL).

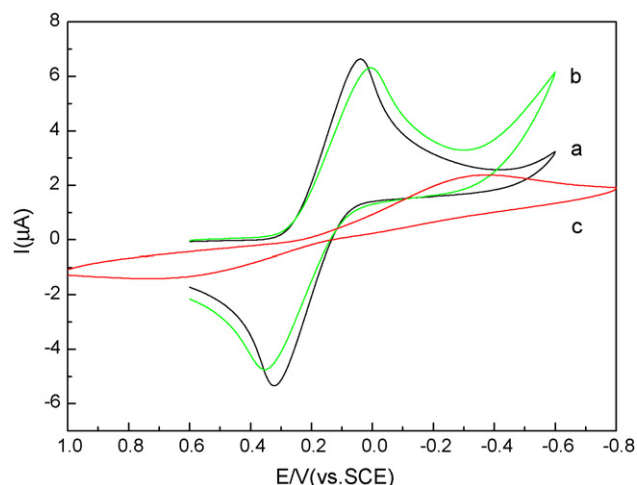


Fig. 4. Cyclic voltammograms of (a) bare ITO, (b) GNSs/APTES/ITO and (c) Hb/GNSs/APTES/ITO electrodes in PBS (pH 7.0) containing 5 mM K<sub>3</sub>[Fe(CN)<sub>6</sub>]. Scan rate, 0.1 V/s.

At the GNSs/APTES/ITO electrode, a little decrease in the redox peak and the  $\Delta E_p$  was widened to 0.35 V, which may be due to the electrostatic repulsion between Fe(CN)<sub>6</sub><sup>3-</sup> or Fe(CN)<sub>6</sub><sup>4-</sup> anion and the negatively charged surface of GNSs. This electrostatic repulsion would hinder the diffusion of ferricyanide toward the electrode interface and slacked the electron-transfer kinetics [35]. And the great widening of  $\Delta E_p$  at the Hb adsorbed GNSs/APTES/ITO electrode mainly ascribes to its large impedance.

Electrochemical impedance spectroscopy was employed to characterize the interfacial properties of ITO electrodes after GNSs modification and Hb adsorption using 10 mM [Fe(CN)<sub>6</sub>]<sup>3-</sup>/[Fe(CN)<sub>6</sub>]<sup>4-</sup> as the redox probe. Fig. 5 shows the impedance spectra in the form of Nyquist diagrams of various ITO electrodes. The diameter of the semicircle usually equals the

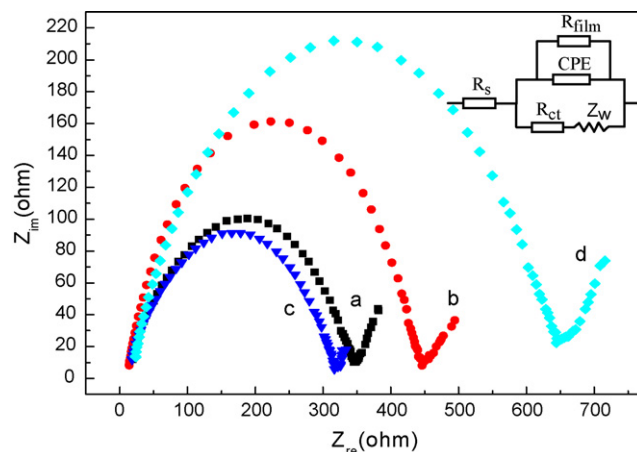


Fig. 5. Electrochemical impedance spectroscopy of (a) bare ITO, (b) APTES/ITO, (c) GNSs/APTES/ITO and (d) Hb/GNSs/APTES/ITO electrodes in 10 mM K<sub>3</sub>Fe(CN)<sub>6</sub>/K<sub>4</sub>Fe(CN)<sub>6</sub> (1:1) containing 0.10 M KCl. Applied potential: 0.19 V; frequency range: 0.1 Hz to 100 kHz. The inset is the Randle's equivalent circuit using a CPE instead of capacitance and adding an additional resistance of modified film parallel to the CPE.

electron-transfer resistance ( $R_{ct}$ ), which controls the electron-transfer kinetics of the redox probe at the electrode interface [36]. When APTES layer was successively adsorbed on the surface of ITO electrode, the electron-transfer resistance ( $R_{ct}$ ) value increased from 347 to 412  $\Omega$ , while decreased to 320  $\Omega$  after GNSs adsorption on the APTES surface due to better conductivity of GNSs, suggesting effectively improved heterogeneous electron-transfer kinetics between the redox couple and electrode interface. After incubation of Hb on the GNSs/APTES/ITO electrode, a semicircle with significantly large diameter was observed, indicating that the adsorbed Hb lead to a great increase in resistance. This effect possibly arises from the insulated polypeptide backbone of the protein.

In addition, the interfacial double-layer capacitance between an electrode and a solution is related to the surface condition of the electrode. Since the surface of the ITO electrode is highly modified, in order to fit the impedance data of the modified electrode, we modified the Randle's circuit model by using a constant phase element (CPE) instead of the classical capacitance, and adding an additional resistance of the modified film ( $R_{film}$ ) parallel to the CPE [37], as shown in the inset of Fig. 5. For bare ITO electrode, there is no  $R_{film}$  element in this case because there is no film present. The additional parameter  $Z_w$  accounts for the Warburg impedance. All parameters of the circuit element were evaluated by fitting the impedance data to the equivalent circuits with data analytical software Zview (data not shown). By comparing the  $R_{film}$  of the GNSs/APTES/ITO electrode ( $R_{film} = 645 \Omega$ , 0.59%) with that of the APTES/ITO electrode ( $R_{film} = 890 \Omega$ , 1.31%), we can infer that the GNSs could effectively decrease the resistance of the modified film.

### 3.3. Direct electrochemical behavior of Hb on GNSs/APTES/ITO electrode

Cyclic voltammograms of different electrodes were measured in PBS (pH 7.0), as shown in Fig. 6. Compared with GNS/APTES/ITO electrode, the Hb/GNS/APTES/ITO electrode gave a couple of well-defined redox peaks at  $-0.21$  and  $-0.32$  V, at a scan rate of 0.1 V/s. These results show that a direct electron transfer process takes place between the adsorbed Hb and the GNS/APTES/ITO electrode. However, as reported in the previous work of Zhang and Oyama [38], no redox peak was observed at the Hb/Au/ITO electrode. This means that compared with gold nanoparticles, GNSs may act as more effective adsorption sites that can penetrate easily to the active center of the Hb molecules. Furthermore, GNSs of the films would provide multiple adsorption sites for Hb molecules, retaining the bioactivity of the adsorbed Hb.

The inset A of Fig. 6 shows the relationship between the peaks current of Hb/GNSs/APTES/ITO electrode and the scan rate. With an increasing scan rate ranging from 50 to 800 mV/s the anodic and cathodic peak potentials of the Hb showed a small shift and the redox peak currents increased linearly, indicating a surface-controlled electrode process. The peak-to-peak separations of the cyclic voltammograms of the Hb/GNSs/APTES/ITO electrode at 100, 200, 300, 400 and 500 mV/s were 110, 111, 113, 115 and 118 mV, respectively. Supposing the charge trans-

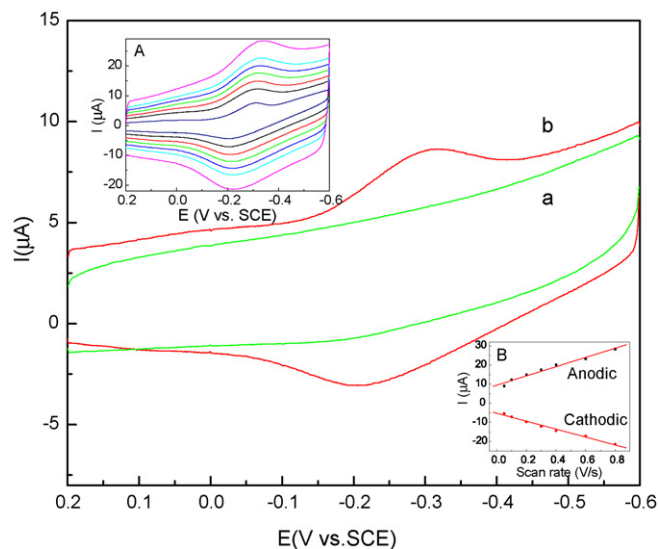


Fig. 6. Cyclic voltammograms of (a) GNSs/APTES/ITO and (b) Hb/GNSs/APTES/ITO electrodes in pH 7.0 PBS at the scan rate of 0.1 V/s. Inset A: Cyclic voltammograms of the Hb/GNSs/APTES/ITO electrode in PBS (pH 7.0) at the scan rates of 0.05, 0.1, 0.2, 0.3, 0.4, 0.5 and 0.8 V/s (from inner to outer). Inset B: Plot of the cathodic and anodic peak currents vs. scan rate.

fer coefficient was between 0.3 and 0.7, the electron transfer rate constant ( $k_s$ ) was estimated to be  $(2.39 \pm 0.7) \text{ s}^{-1}$  according to Laviron's model with the formula  $k_s = mnFv/RT$  [39], where  $m$  is a parameter related to the peak-to-peak separation. This value is significantly higher than the  $0.49 \text{ s}^{-1}$  at the Hb/GNPs/cystamin/Au electrode as reported previously [40], suggesting a reasonably fast electron transfer between the immobilized Hb and the electrode ascribed to the presence of GNSs.

### 3.4. Electrocatalysis of Hb/GNSs/APTES/ITO electrode toward $\text{H}_2\text{O}_2$

Cyclic voltammograms of the Hb/GNSs/APTES/ITO before and after injection of 0.6 mM  $\text{H}_2\text{O}_2$  solution in pH 7.0 PBS were shown in Fig. 7A. After addition of  $\text{H}_2\text{O}_2$ , an increase in reduction current for the Hb/GNSs/APTES/ITO electrode could be observed when the potential is lower than  $-0.1$  V. This phenomenon was not observed clearly at a bare ITO or a GNSs/APTES/ITO electrode. Thus, the catalysis reduction of  $\text{H}_2\text{O}_2$  was ascribed to the presence of Hb.

The chronoamperometric curve is recorded on Hb/GNSs/APTES/ITO electrode under the conditions of continuous stirring of the solution and successive injection of aliquot  $\text{H}_2\text{O}_2$  at  $-0.25$  V (as shown in Fig. 7B). As the  $\text{H}_2\text{O}_2$  was added into the stirring buffer solution, the biosensor responded rapidly to the substrates. The inset b of Fig. 7B exhibits the plot of catalytic current of the Hb/GNSs/APTES/ITO electrode versus  $\text{H}_2\text{O}_2$  concentration. A good linear relationship is found between the catalytic current and  $\text{H}_2\text{O}_2$  concentration from  $5 \times 10^{-6}$  to  $1.0 \times 10^{-3}$  M. The linear regression equation is expressed as  $y = 1.547x + 2.981 \mu\text{A}$ , with a correlation coefficient of 0.999 ( $n = 14$ ). The detection limit ( $S/N = 3$ ) is estimated to be  $3.4 \mu\text{M}$ . When the concentration of  $\text{H}_2\text{O}_2$  is higher than 1.0 mM, a platform emerges in the catalytic peak current, showing the

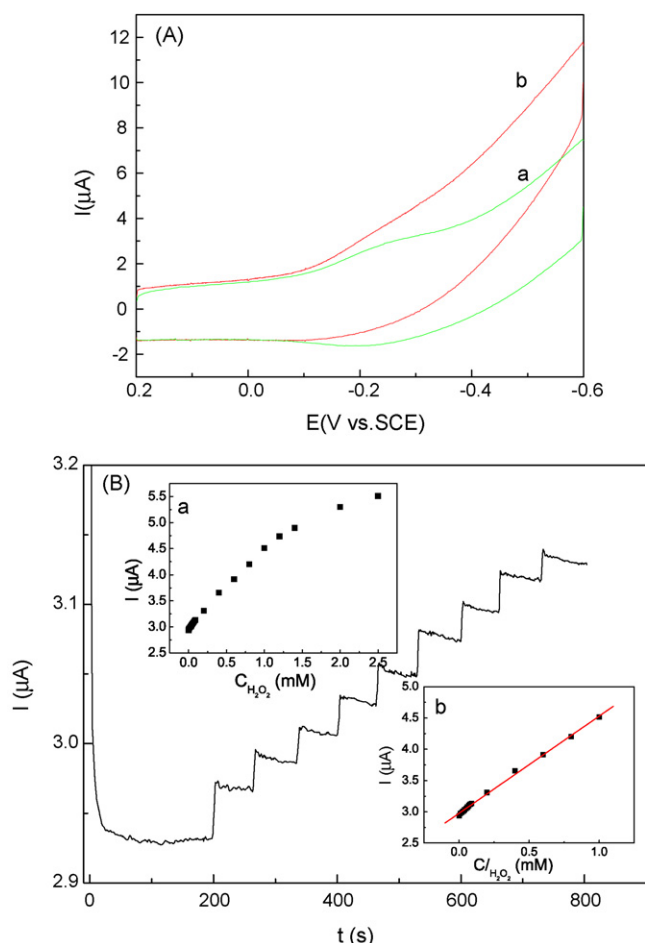


Fig. 7. (A) Cyclic voltammograms of the Hb/GNSs/APTES/ITO electrode in pH 7.0 PBS (a) without and (b) with 0.6 mM  $\text{H}_2\text{O}_2$  at the scan rate of 50 mV/s. (B) Chronoamperometric responses observed at the Hb/GNSs/APTES/ITO electrode in 0.1 M PBS (pH 7.0) after successively injecting 0.01 mM  $\text{H}_2\text{O}_2$ . Applied potential:  $-0.25$  V. Inset a: Plot of catalytic current vs.  $\text{H}_2\text{O}_2$  concentration. Inset b: Linear calibration curve of the biosensor.

characteristics of Michaelis–Menten kinetics. The apparent Michaelis–Menten constant ( $K_m^{\text{app}}$ ), which gives an indication of the enzyme–substrate kinetics, is 0.18 mM as calculated by the Lineweaver–Burk equation  $1/I_{\text{ss}} = 1/I_{\text{max}} + K_m^{\text{app}}/I_{\text{max}}C$  [41], where  $I_{\text{ss}}$ ,  $I_{\text{max}}$  and  $C$  stand for steady state current, maximum current and  $\text{H}_2\text{O}_2$  concentration, respectively. It is well known that a smaller  $K_m^{\text{app}}$  represents a higher catalytic ability. Since this is smaller than the 0.31 mM obtained at Hb/ZrO<sub>2</sub>/DMSO/PG [34], 1.4 mM at Hb/Chit-Aus/Cys/Au [42], 1.30 mM at Mb-silver NPs/PG [43] and 0.2 mM at Cyto-c/nano-LTL-zeolite/ITO electrode [44], it is indicated that Hb immobilized on GNSs is of a higher affinity to  $\text{H}_2\text{O}_2$ .

### 3.5. Stability and reproducibility of the modified electrode

To evaluate the stability and reproducibility of the electrode, the Hb/GNSs/APTES/ITO electrode was stored in PBS at 4 °C when it was not in use. It remained 90% of its initial catalytic current after 3 weeks storage. The response of a Hb/GNSs/APTES/ITO electrode was examined for six measurements in 0.6 mM  $\text{H}_2\text{O}_2$  in pH 7.0 PBS, and the catalytic current

at  $-0.25$  V shows a relative standard deviation (R.S.D.) of 4.5%. The fabrication of five electrodes, made independently with the same bare electrode, showed an acceptable reproducibility with a R.S.D. value of 5.6% for the catalytic current at  $-0.25$  V in pH 7.0 PBS with 0.6 mM  $\text{H}_2\text{O}_2$ .

## 4. Conclusion

GNSs/APTES/ITO electrodes were successfully constructed by self-assembly of GNSs on ITO substrates. The results of UV–vis spectra showed that Hb retained its native structure after its adsorption on these electrodes, which may be ascribed to the high surface area and good biocompatibility of GNSs. The self-assembly of GNSs onto the electrode surface provided the necessary conduction pathways and allowed efficient electron tunneling, which realized the direct electron transfer from Hb to the electrode surface. And a couple of well-defined redox peaks can be observed at the Hb/GNSs/APTES/ITO electrode. In addition, the resulted Hb/GNSs/APTES/ITO electrode exhibited excellent electrocatalytic properties toward the reduction of  $\text{H}_2\text{O}_2$ , low detection limit and broad linear range. Compared with GNPs, GNSs may provide more effective adsorption sites that can be accessed easily to the active center of adsorbed protein molecules. Therefore, the GNSs interface architecture offers an opportunity for obtaining high-quality detectors for bioelectroanalysis, capillary electrophoresis, miniaturized total analysis systems and other fields.

## Acknowledgments

This research is supported by the National Nature Science Foundation of China (no. 20475009, 90406024-4, 60121101), the Nature Science Foundation from Jiangsu province, the Foundation from the Ministry of Education, and the Foundation for the Author of National Excellent Doctoral Dissertation of PR China (No. 200252).

## References

- [1] S. Haymond, G.T. Babcock, G.M. Swain, *J. Am. Chem. Soc.* 124 (2002) 10634.
- [2] T. Liu, J. Zhong, X. Gan, C. Fan, G. Li, N. Matsuda, *Chem. Phys. Chem.* 4 (2003) 1364.
- [3] H.Y. Liu, N.F. Hu, *J. Phys. Chem. B* 109 (2005) 10464.
- [4] E. Topoglidis, Y. Astuti, F. Duriaux, M. Grätzel, J.R. Durrant, *Langmuir* 19 (2003) 6894.
- [5] C. Wang, C. Yang, Y. Song, W. Gao, X. Xia, *Adv. Funct. Mater.* 15 (2005) 1267.
- [6] A. Liu, M. Wei, I. Honma, H. Zhou, *Anal. Chem.* 77 (2005) 8068.
- [7] C.E. Immoos, J. Chou, M. Bayachou, E. Blair, J. Greaves, P.J. Farmer, *J. Am. Chem. Soc.* 126 (2004) 4934.
- [8] S. Liu, A. Chen, *Langmuir* 21 (2005) 8409.
- [9] L. Wang, E.K. Wang, *Electrochem. Commun.* 6 (2004) 225.
- [10] R. Hirsch, E. Katz, I. Willner, *J. Am. Chem. Soc.* 122 (2000) 12053.
- [11] H. Zhou, X. Gan, J. Wang, X. Zhu, G. Li, *Anal. Chem.* 77 (2005) 6102.
- [12] Y. Xiao, F. Patolsky, E. Katz, J.F. Hainfeld, I. Willner, *Science* 299 (2003) 1877.
- [13] A. Yu, Z. Liang, J. Cho, F. Caruso, *Nano Lett.* 3 (2003) 1203.
- [14] R. Szamocki, S. Reculosa, S. Ravaine, P.N. Bartlett, A. Kuhn, R. Hempelmann, *Angew. Chem. Int. Ed.* 45 (2006) 1317.

- [15] P.L. He, N.F. Hu, *Electroanalysis* 16 (2004) 1122.
- [16] S.R. Sershen, N.J. Halas, J.L. West, *J. Biomed. Mater. Res.* 51 (2000) 293.
- [17] A.M. Gobin, D.P. O'Neal, D.M. Watkins, N.J. Halas, R.A. Drezek, J.L. West, *Lasers Surg. Med.* 37 (2005) 123.
- [18] Y. Wang, X. Xie, X. Wang, G. Ku, K.L. Gill, D.P. O'Neal, G. Stoica, L.V. Wang, *Nano Lett.* 4 (2004) 1689.
- [19] C. Loo, A. Lowery, N. Halas, J. West, R. Drezek, *Nano Lett.* 5 (2005) 705.
- [20] J.B. Jackson, N.J. Halas, *Proc. Natl. Acad. Sci. U.S.A.* 101 (2004) 17930.
- [21] L.R. Hirsch, J.B. Jackson, A. Lee, N.J. Halas, J.L. West, *Anal. Chem.* 75 (2003) 2377.
- [22] S.J. Oldenburg, R.D. Averitt, S.L. Westcott, N.J. Halas, *Chem. Phys. Lett.* 288 (1998) 243.
- [23] Y. Tan, S. Ding, Y. Wang, W. Qian, *Acta Chim. Sin.* 63 (2005) 929.
- [24] Y. Wang, Y. Tan, S. Ding, L. Li, W. Qian, *Acta Chim. Sin.* 64 (2006) 2291.
- [25] S. Ding, W. Qian, Y. Tan, Y. Wang, *Langmuir* 22 (2006) 7105.
- [26] Y. Tan, W. Qian, S. Ding, Y. Wang, *Chem. Mater.* 18 (2006) 3385.
- [27] H.A. Kozłowska, B.E. Conway, A. Hamelin, L. Stoicoviciu, *J. Electroanal. Chem.* 278 (1987) 429.
- [28] P. George, G. Hanania, *Biochem. J.* 55 (1953) 236.
- [29] A.E.F. Nassar, W.S. Willis, J.F. Rusling, *Anal. Chem.* 67 (1995) 2386.
- [30] N. Jia, Q. Zhou, L. Liu, M. Yan, Z.Y. Jiang, *J. Electroanal. Chem.* 580 (2005) 213.
- [31] H. Yao, N. Li, J.Z. Xu, J.J. Zhu, *Talanta*, in press.
- [32] Y. Xu, F. Wang, X. Chen, S. Hu, *Talanta* 70 (2006) 651.
- [33] S. Liu, Z. Dai, H. Chen, H. Ju, *Biosens. Bioelectron.* 19 (2004) 963.
- [34] X. Lu, Q. Zhang, L. Zhang, J. Li, *Electrochem. Commun.* 8 (2006) 874.
- [35] S. Zhang, N. Wang, H. Yu, Y. Niu, C. Sun, *Bioelectrochemistry* 67 (2005) 15.
- [36] E. Katz, I. Willner, *Electroanalysis* 15 (2003) 913.
- [37] L.V. Protsailo, W.R. Fawcett, *Electrochim. Acta* 45 (2000) 3497.
- [38] J. Zhang, M. Oyama, *Electrochim. Acta* 50 (2004) 85.
- [39] E. Laviron, *J. Electroanal. Chem.* 101 (1979) 19.
- [40] H.Y. Gu, A.M. Yu, H.Y. Chen, *J. Electroanal. Chem.* 516 (2001) 119.
- [41] R.A. Kamin, G.S. Wilson, *Anal. Chem.* 52 (1980) 1198.
- [42] J.J. Feng, G. Zhao, J.J. Xu, H.Y. Chen, *Anal. Biochem.* 342 (2005) 280.
- [43] X. Gan, T. Liu, J. Zhong, X. Liu, G. Li, *Chem. Biol. Chem.* 5 (2004) 1686.
- [44] T. Yu, Y. Zhang, C. You, J. Zhuang, B. Wang, B. Liu, Y. Kang, Y. Tang, *Chem. Eur. J.* 12 (2006) 1137.